Ancestral genetic diversity associated with the rapid spread of stress-tolerant coral symbionts in response to Holocene climate change

Benjamin C. C. Hume[a], Christian R. Voolstra[b], Chatchanit Arif[b], Cecilia D'Angelo[a,c], John A. Burt[d], Gal Eyal[e,f], Yossi Loya[e], and Jörg Wiedenmann[a,c,1]

[a]Coral Reef Laboratory, Ocean and Earth Science, University of Southampton, Southampton SO14 3ZH, United Kingdom; [b]Red Sea Research Center, Division of Biological and Environmental Science and Engineering, King Abdullah University of Science and Technology (KAUST), Thuwal 23955-6900, Saudi Arabia; [c]Institute for Life Sciences, University of Southampton, Southampton SO17 1BJ, United Kingdom; [d]Marine Biology Laboratory, Centre for Genomics and Systems Biology, New York University Abu Dhabi, Abu Dhabi 129188, United Arab Emirates; [e]Department of Zoology, Tel Aviv University, Tel Aviv 6997801, Israel; and [f]The Interuniversity Institute for Marine Sciences in Eilat, Eilat 8810369, Israel

Edited by Nancy Knowlton, Smithsonian Institution, Washington, DC, and approved March 3, 2016 (received for review February 4, 2016)

Coral communities in the Persian/Arabian Gulf (PAG) withstand unusually high salinity levels and regular summer temperature maxima of up to ∼35 °C that kill conspecifics elsewhere. Due to the recent formation of the PAG and its subsequent shift to a hot climate, these corals have had only <6,000 y to adapt to these extreme conditions and can therefore inform on how coral reefs may respond to global warming. One key to coral survival in the world's warmest reefs are symbioses with a newly discovered alga, *Symbiodinium thermophilum*. Currently, it is unknown whether this symbiont originated elsewhere or emerged from unexpectedly fast evolution catalyzed by the extreme environment. Analyzing genetic diversity of symbiotic algae across >5,000 km of the PAG, the Gulf of Oman, and the Red Sea coastline, we show that *S. thermophilum* is a member of a highly diverse, ancient group of symbionts cryptically distributed outside the PAG. We argue that the adjustment to temperature extremes by PAG corals was facilitated by the positive selection of preadapted symbionts. Our findings suggest that maintaining the largest possible pool of potentially stress-tolerant genotypes by protecting existing biodiversity is crucial to promote rapid adaptation to present-day climate change, not only for coral reefs, but for ecosystems in general.

Persian/Arabian Gulf | adaptation | coral | *Symbiodinium* | climate change

Episodes of heat stress cause coral bleaching, the breakdown of the obligate symbiosis between the coral host and its algal partner that contributes to the global decline of coral reefs (1). Despite their capacity to acclimate to rising seawater temperatures (2), corals will suffer from high-frequency bleaching episodes by the end of this century, threatening their survival in the warmer oceans of the future (3). Changing to symbiotic associations with more thermally tolerant types like *Symbiodinium trenchii* (synonym type D1a/D1–4) may increase the heat stress tolerance of corals rapidly (4–6). However, due to tradeoffs such as reduced calcification rates that can be associated with hosting alternative symbionts, reef ecosystems may ultimately fail to benefit from the increased thermal tolerance of their most important habitat-forming species (5, 6). Hence, it is unclear at present whether alternative symbiont associations will rescue reefs from their expected demise in response to global warming.

We are using the Persian/Arabian Gulf (PAG), the world's hottest sea, as a natural laboratory where coral communities endure regular summer temperatures of up to ∼35 °C to address the question of how coral reefs relying on heat-tolerant *Symbiodinium* may respond to rapid climate change over a prolonged period. Due to rising sea levels associated with the last glacial retreat, the modern PAG started to form ∼12,500 y before present (BP) by ingression of the Indian Ocean into the previously dry basin, extending to present-day shorelines ∼6,000 y BP (7). By this time, the climate in the Middle East began to change from cooler and moister to warmer and more arid, reaching today's conditions only ∼4,000 y ago (8–10). Hence, the coral communities of the PAG, composed mostly of a subset of Indian Ocean species (11), have had to adjust rapidly to temperatures not expected to occur in other parts of the world's oceans before the next century (12). We recently discovered that corals of the southern, hottest region of the PAG form a prevalent, year-round association with a thermally tolerant symbiont species, *Symbiodinium thermophilum* (13). Although the symbiosis with *S. thermophilum* might not be the sole cause for the heat tolerance, and others factors including the host physiology (14) and environmental conditions (such as the exceptionally high salinity in the relevant PAG regions) (15) may contribute to the resilience of the holobiont, the striking dominance of this symbiont in the southern PAG strongly suggests that it represents a key component to the success of corals in this extreme environment.

S. thermophilum can be identified by specific intragenomic variants of the nuclear ribosomal second internal transcribed spacer region (ITS2), which carry an 8-bp duplication indel named "*S. thermo.*-indel" (13). In close to pure *S. thermophilum* populations, these variants represent an average ∼16% of the total

Significance

Reef corals in the Persian/Arabian Gulf (PAG) withstand exceptionally high salinity and regular summer temperatures of ∼35 °C that kill conspecifics elsewhere. These thermotolerant communities established themselves within only ∼6,000 y under the pressure of rapid climate change and can therefore inform how other coral reefs may respond to global warming. One key to the thermotolerance of PAG corals is their symbiosis with *Symbiodinium thermophilum*. Phylogeographic evidence indicates that this symbiont represents a stress-tolerant subpopulation of an ancestral taxonomic group with surprising genetic diversity that exists at barely detectable levels outside the PAG. Our results highlight the critical importance of present-day biodiversity for future adaptation to climate change for coral reefs and ecosystems in general.

Author contributions: B.C.C.H., C.R.V., and J.W. designed research; B.C.C.H., C.R.V., and C.A. performed research; B.C.C.H., C.R.V., J.A.B., G.E., Y.L., and J.W. performed field work; B.C.C.H., C.R.V., C.A., C.D., and J.W. analyzed data; and B.C.C.H., C.D., and J.W. wrote the paper.

The authors declare no conflict of interest.

This article is a PNAS Direct Submission.

Freely available online through the PNAS open access option.

Data deposition: The sequences reported in this paper have been deposited in the GenBank database (accession nos. KR996268–KR996464 and KT156647–KT156665).

[1]To whom correspondence should be addressed. Email: joerg.wiedenmann@noc.soton.ac.uk.

This article contains supporting information online at www.pnas.org/lookup/suppl/doi:10.1073/pnas.1601910113/-/DCSupplemental.

ITS2 sequences, however this proportion can vary considerably (Fig. S1). Additionally, this symbiont can be distinguished by its genetically disparate resolution from other closely related ITS2 C3 types using the noncoding region of the chloroplastic *psbA* gene (*psbA*^{ncr}) among other markers (13). As yet undetected in other parts of the world, our previous work suggested that symbionts characterized by the *S. thermo.*-indel and a disparate *psbA*^{ncr} resolution (hereafter *S. thermophilum* group) may not be endemic to the PAG (15). Because the understanding of heat tolerance in coral–symbiont associations is crucial in gauging the adaptation potential of coral reefs to global warming, we investigated the origin of *S. thermophilum* to assess whether this thermotolerant symbiont emerged as the result of an unexpectedly rapid evolution under the pressure of the extreme environmental conditions in the PAG or whether this species originated elsewhere.

Results and Discussion

We screened for *S. thermophilum* at 23 sites across >5,000 km of coastline from the northwestern PAG to the Gulf of Eilat/Aqaba in the Red Sea (Fig. 1*A*). The symbiont was detected by the presence of the *S. thermo.*-indel in libraries containing 2.8 × 10^6 ITS2 amplicons obtained by 454 and MiSeq sequencing (except

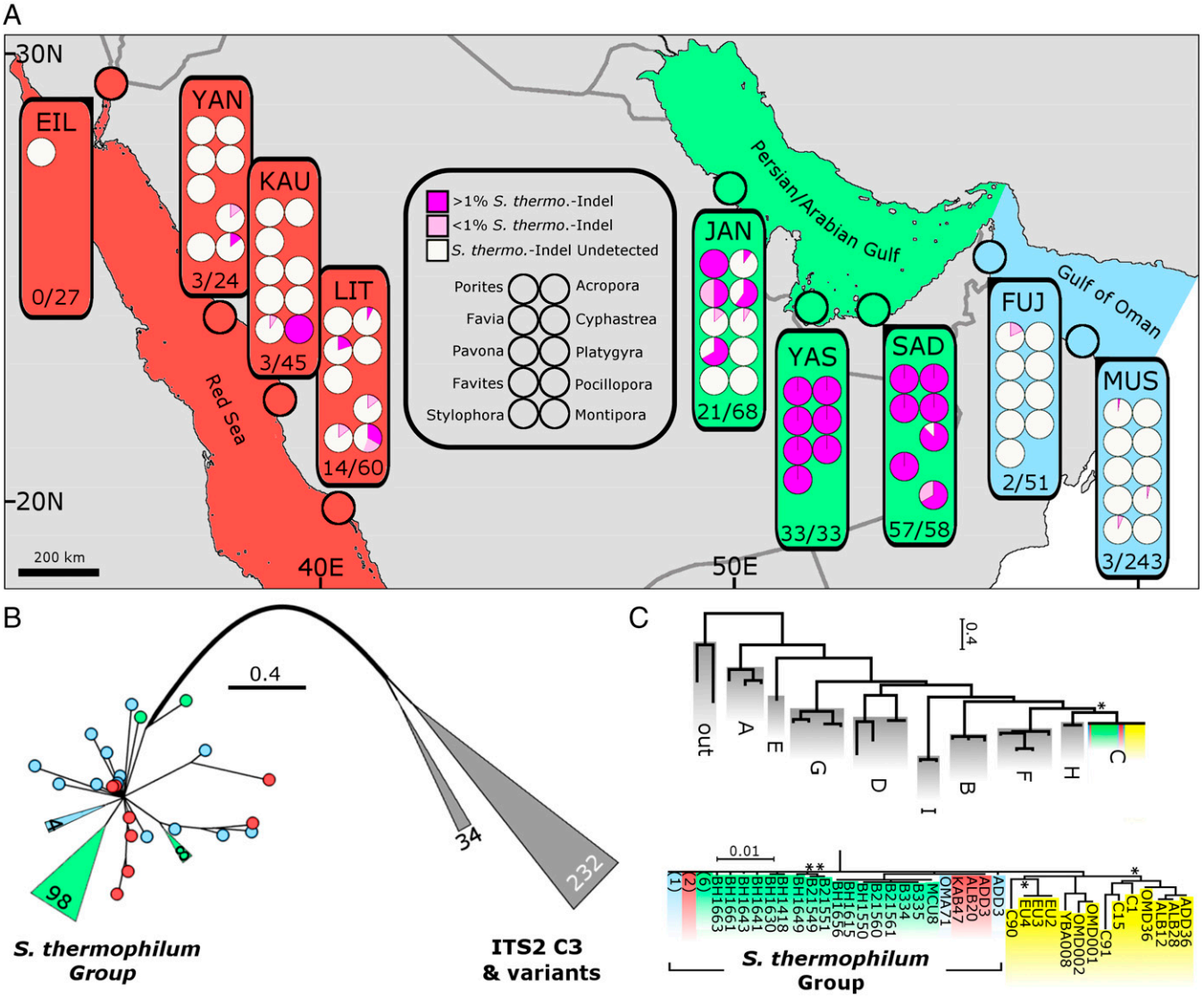

Fig. 1. Identification and phylogenetic resolution of the *S. thermophilum* group. Colors denote sampling locations according to map coloration with yellow denoting non-*S. thermophilum* group clade C symbionts. (*A*) Sampling sites (three letter abbreviations; e.g., JAN) are detailed in Table S1. The presence of *S. thermophilum* group symbionts within the 10 most sampled genera are presented categorically (undetected, <1% and >1% *S. thermo.*-indel). Regional summaries (*)/(*) represent the proportion of samples in which *S. thermophilum* group symbionts were detected (Tables S1 and S2). The map was created as detailed in Hume et al., 2015 (13). (*B*) *PsbA*^{ncr} estimated phylogeny of *S. thermophilum* group samples created through the addition of samples collected in the Gulf of Oman and the Red Sea (sequenced as part of this study) to *psbA*^{ncr} alignments previously constructed (15). Symbionts within the gray branches are ITS2 type C3 and closely related ITS2 types from the Atlantic and Indo-Pacific (17). Wedges and circles represent collapsed groups and individual samples, respectively. Lengths of collapsed branches are drawn to scale with number of contained sequences indicated. (*C*) Supermatrix Bayesian estimation of phylogeny using six additional genetic markers (Fig. S3 and Table S5) on a selection of cnidarian-harbored *Symbiodinium* samples collected in the PAG, the Gulf of Oman, the Red Sea, as well as several reference locations (see *Methods* for further details). The full collapsed tree with clade C subtree is expanded below. Numbers in parentheses represent multiple sequences resolving at the same position and are colored according to collection site and sequence type (Gulf of Oman, blue; PAG, green; Red Sea, red; reference sequences, yellow). Gray groupings contain reference *Symbiodinium* from clades A–I as well as two outgroups (*G. simplex and P. glacialis*) (Table S5). Nodes supported with posterior probability (PP) above 0.8 are not displayed. Nodes with supports below 0.8 are marked with an asterisk (*).

Eilat; see *Methods*) of >900 symbiotic hexa- and octocorallians from 46 genera (Tables S1 and S2). The results for the 10 most sampled taxa are presented in Fig. 1*A*, with details being given for all samples in Fig. 2 and Tables S1 and S2.

Members of the *S. thermophilum* group were found in 10 out of the 11 sampled genera in the southern PAG but were less frequent in the western PAG and could only be detected at low levels in ~4% of samples in the Gulf of Oman and the Red Sea (Figs. 1 and 2 and Tables S1 and S2). Additionally, when screening public databases for ITS2 sequences containing the *S. thermo.*-indel, we retrieved a close match with a sequence originating from Kaneohe Bay, Hawaii, which was recently entered in GenBank (accession no. EF428343). This hit may indicate the presence of a *S. thermophilum* group member in the Indo-Pacific, implying an even wider, cryptic distribution.

PsbA^{ncr} sequences of samples containing the *S. thermo.*-indel from the Gulf of Oman and Red Sea are resolved within the strongly supported (PP = 1) monophyletic *S. thermophilum* group (Fig. 1*B* and Table S3) but as genetically separate from the majority of PAG sequences and with larger average within-group genetic distances (0.065 vs. 0.039; Table S4). The average genetic distance of the five most divergent sequence pairs within the *S. thermophilum* group was larger than that between the considerably divergent C27 and C40 ITS2 types (0.163 vs. 0.154; Fig. S2 and Table S4), demonstrating a genetic diversity in the group greater than that found among considerably divergent clade C lineages. This highlights the existence of a wide range of previously unidentified and possibly stress-tolerant genotypes within the group.

To establish the age and taxonomic position of the *S. thermophilum* group within clade C, we estimated molecular phylogenies of this group with representatives from *Symbiodinium* clades A–I, including subclade C representatives, using a suite of single gene markers (Tables S3 and S5) through Bayesian analysis. These markers varied in their ability to resolve between clade C types (Fig. S3 and Table S6). Nine of the 31 *S. thermophilum* group samples showed identical resolutions across all markers and resolved on the ancestral node in a supermatrix phylogeny (Fig. 1*C*). All non-*S. thermophilum* group samples resolved as a strongly supported monophyletic group derived from this ancestral node, whereas those *S. thermophilum* group samples not resolved on the ancestral node separated as sister groups or individual samples. Given the molecular dating of the radiation of clade C placed in the mid-Miocene, these results provide strong evidence that the *S. thermophilum* group represents one of the oldest (~13 Mya) and most genetically diverse groups of extant clade C symbionts (16). Furthermore, estimation of divergences between lineages within the ITS2 type C3 and closely related ITS2 variants according to the *psbA*^{ncr} as being between 2 and 12 My old (17), would suggest that within-group genetic distances of the *S. thermophilum* group represent evolutionary divergences occurring over at least several million years, a span considerably longer than the age of the PAG (Fig. S2).

The diversity of S. *thermophilum–psbA*^{ncr} was assessed by analyzing sequences from independent samples (Table S7) representing six sites in the PAG and nine sites in the Gulf of Oman and the Red Sea. The significant difference (two-sample *t* test, *P* value < 0.01) obtained for group comparisons between within-group genetic distances of PAG sequences (0.039; 112 samples) and Gulf of Oman/Red Sea sequences (0.065; 22 samples) (Table S4) provides evidence that the genetic diversity of *S. thermophilum* in the PAG is strongly reduced compared with the sites outside of this water body. Similarly, in the southern PAG, the overall *Symbiodinium* diversity at the species/clade level is lower compared with the western PAG and the Strait of Hormuz, which connects the PAG with the Gulf of Oman (15, 18) (Figs. 1*A* and 2).

The low genetic diversity of the *S. thermophilum* population in the southern PAG could be indicative of a recent bottleneck event or a founder effect. However, the PAG is well connected to the Gulf of Oman via the dominant inflow of surface water through the Strait of Hormuz (18), and various symbiont types including *S. trenchii* (synonym type D1a/D1-4), some of which are known to be heat stress-tolerant and to associate with many different coral species (19), are already established in other regions of the PAG and the Strait of Hormuz (15). Together with the fact that *Symbiodinium* can disperse rapidly over long distances (6, 19, 20), these conditions should promote a rapid homogenization of the symbiont distribution. Hence, the distinct distribution patterns presented in this study render founder or bottleneck effects rather unlikely causes of the low genetic diversity of *S. thermophilum* in the southern PAG. More plausibly, the genetic uniformity of this symbiont in the hottest coral reef ecosystem in the world may have resulted from a strong positive selection of a few of the most thermally tolerant genotypes from an old lineage with a more widespread but cryptic distribution. This selection pressure may not have resulted only from temperature extremes in the southern PAG, but might also have been influenced by the

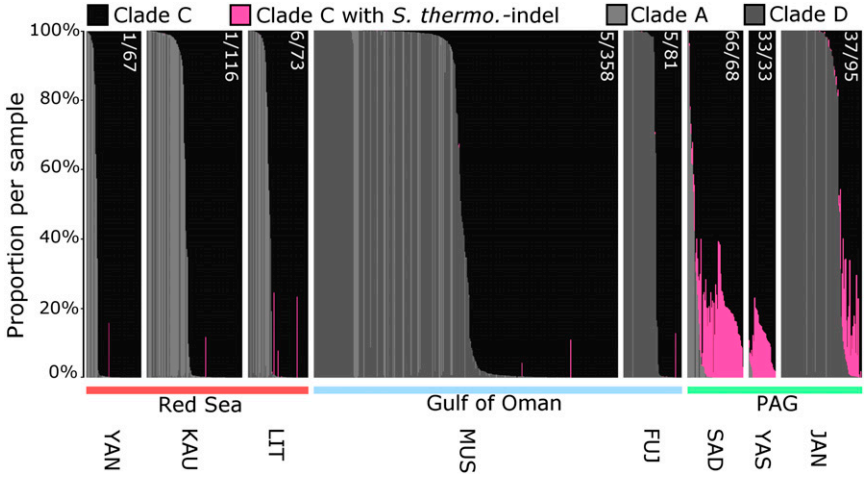

Fig. 2. Identification of clade C sequences containing the *S. thermo.*-indel as a proxy for the presence of *S. thermophilum* and classification of the symbiont complements in all sampled individuals. Each vertical bar represents a single sample. The contribution of sequences representing different clades/species to the sequence complement of each sample is color-coded as defined in the legend. Sample origins are shown below the chart (Table S1). Numbers of samples containing the *S. thermo.*-indel as a proportion of the total samples are shown in white in the format (*)/(*) (Tables S1 and S2).

exceptionally high salinity of this habitat (15). Moreover, it cannot be ruled out that characteristics of today's *S. thermophilum* populations were recently influenced by evolutionary processes despite the relatively short time (~thousands of years) that this symbiont has been exposed to the pressures of the PAG environment.

A contrasting scenario was recently presented for the Caribbean, where the lack of genetic diversity among thermotolerant *S. trenchii* was interpreted as an indicator of a recent, long-range introduction of coral symbiont species (6). There, the opportunistic/invasive nature of a small founder population promoted its rapid spread to coral communities across the Greater Caribbean.

Although productive coral ecosystems exist in the southern PAG, the diversity of its habitat-forming scleractinian corals (34 species) (21) is substantially lower compared with the adjacent Gulf of Oman (68 species) (11) and the central and northern Red Sea (289 species) (22). Furthermore, in contrast to many other parts of the world, where corals construct reefs by forming vertically growing platforms through calcium carbonate accretion, corals in the southern PAG form only a living veneer over suitable substrates (8). Applying the findings from the PAG to the future of coral reefs elsewhere, it appears that coral–dinoflagellate symbioses may respond rapidly to increasing water temperature by the spread of tolerant symbiont associations, which are normally ecologically rare. Nonetheless, the PAG ecosystem has had millennia to adapt, whereas the adaptation to global warming will need to take place over decades to centuries. As exemplified by the coral communities of the PAG and changes in their composition in response to short-term temperature anomalies, not all species will survive beyond certain changes in the environment (21, 23). Inevitably, the shift toward more extreme environmental conditions on the global scale will be accompanied by a substantial loss of diversity both at the species and within-species level.

Although the failure of corals to build reefs in the PAG has been previously attributed to high-frequency disturbances, high-level bioerosion, and the constant exposure of corals to temperature and salinity extremes (8, 15, 24), the dominance of thermally tolerant coral–dinoflagellate combinations might also contribute to reduced reef accretion as recently exemplified for coral communities elsewhere (4–6). Because modeling predicts that reef accretion will not easily keep up with projected rates of sea-level rise at present day's growth rates (25), the question arises whether the thermal adaptation of reef corals might come at the cost of an increased risk of reefs drowning in the rising oceans of the future.

Despite the potential tradeoffs that might be associated with the thermal adaptation of coral communities, the example of the PAG suggests that protecting present-day biodiversity is of upmost importance to provide the largest possible genepool from which more stress-tolerant species and genotypes may emerge and become more common under severe natural selection (26, 27). For coral reef ecosystems, this implies that any loss of biodiversity by causes other than heat stress including habitat destruction, pollution, and eutrophication (28–31) will reduce their likelihood of adapting to climate change.

Methods

Collection and DNA Extraction of Samples. Cnidarian samples from 46 genera were collected at 23 reefs in the PAG, the Gulf of Oman, and the Red Sea. Sampling locations were categorized as follows: water bodies (the PAG, the Gulf of Oman, and the Red Sea), sampling regions (made up of one or more reef), and reefs. A detailed list of the sampling locations and number of cnidarians collected at each site can be found in Table S1. All samples were collected by SCUBA (self-contained underwater breathing apparatus) diving with ~1 cm^2 of tissue sampled from the surface of each cnidarian. Samples collected at Eilat were placed into 5 mL of RNAlater, whereas all other samples were flash-frozen in liquid nitrogen before storage at –20 °C.

Genomic DNA (gDNA) was extracted as described for environmental samples in Arif et al., 2014 (32), except for samples collected at Eilat. For Eilat samples, host and symbiont gDNA was extracted using a cetyl trimethylammonium bromide (CTAB) extraction. Before extraction, each of the samples was washed with 96% (vol/vol) ethanol to remove the majority of RNAlater storage buffer to minimize coprecipitation of salts during the DNA precipitation step of the extraction. Samples were then frozen in liquid nitrogen before being added to 1 mL of CTAB extraction buffer [2% (wt/vol) CTAB; 1.4 M NaCl; 0.5% 2-β-mercaptoethanol; 2% (wt/vol) polyvinylpyrrolidone (PVP); 20 mM EDTA; 100 mM Tris·HCl, pH 8.0] and beaten using a 5-mm stainless steel ball in a Tissue Lyser II (Qiagen) at maximum speed until the sample was completely homogenized. Samples were incubated at 60 °C for 30 min before three extractions in 1 mL of chloroform: isoamyl alcohol (IAA) (24:1), phenol:chloroform:IAA (25:24:1), and chloroform:IAA (24:1) with centrifugation after each extraction. The supernatant was added to an equal volume of isopropanol before incubation at –20 °C for 2 h. The DNA was pelleted through centrifugation before being washed in 750 μL of 96% ethanol and centrifuged. Supernatant was removed and pellets were dried before suspension in 50 μL of ddH_2O. All centrifugation steps were carried out at 20,000 × *g* for 5 min at 4 °C.

ITS2 Genotyping of *Symbiodinium* spp. Harbored by Coral Samples. The *Symbiodinium* nuclear ribosomal ITS2 region of all samples except those collected at Eilat was sequenced by 454 and MiSeq sequencing as detailed (32). The *Symbiodinium* ITS2 region of the Eilat-collected samples was sequenced by direct PCR sequencing (services provided by Eurofins MWG) using the internal primer SYM_VAR5.8SII (13) on the 18S-ITS1-5.8S-ITS2-28S amplicon amplified by SYM_VAR-FWD and SYM_VAR_REV as detailed (33), with the exception of an annealing temperature of 56 °C. Results of this sequencing revealed a mix of C15-cluster ITS2 sequences. Given that *S. thermophilum* group symbionts are characterized by an ITS2 type C3, these samples were excluded from further analysis.

Screening of Corals for Associations with *S. thermophilum* Group. To identify the presence of *S. thermophilum* group symbionts, all corals were screened for the characteristic 8-bp indel sequence described in Hume et al., 2015 (13). To incorporate the possibility of PCR error and the existence of possible genetic variants, sequences 1 bp different (substitution only) from the originally described 8-bp sequences were also included in the results (hereafter referred to as the *S. thermo.*-indel) as indicative of the *S. thermophilum* group. Symbiont complements identified as having at least one ITS2 amplicon containing the *S. thermo.*-indel (hereafter referred to as *S. thermo.*-indel amplicons) were further categorized according to whether such amplicons made up more than or less than 1% of the total *Symbiodinium* amplicon sequences found in that organism (Fig. 1*A*). *S. thermo.*-indel–containing amplicons made up between 2% and 41% of the C3 type ITS2 amplicons in *S. thermophilum* samples (i.e., a coral sample hosting 100% *S. thermophilum* would likely have between 2% and 41% ITS2 amplicons containing the *S. thermo.*-indel; Fig. S1). As such, the 1% cutoff used in this study could potentially represent a 50% complement of *S. thermophilum* group symbionts, whereas symbionts containing >15% have a high likelihood of containing a close to pure complement of an *S. thermophilum* group symbiont.

Verification of *S. thermophilum* Group by PCR Amplification, Sequencing, and Phylogenetic Analysis of the *psbA^{ncr}*. To validate the successful identification of the *S. thermophilum* group by the presence of the *S. thermo.*-indel, samples from the Gulf of Oman and Red Sea that contained more than 25% clade C ITS2 sequences and in which *S. thermo.*-indel amplicons made up more than 1% of the clade C sequences had the *psbA^{ncr}* analyzed by direct PCR sequencing as detailed in Hume et al., 2015 (13). Chromatograms were checked manually for miscalls. Chromatograms with multiple peaks were first assessed to determine whether the multiple peaks could be explained by a reading frame shift caused by indels by calling secondary peaks using the software Geneious 5.1.7 (www.geneious.com) before attempting to resolve indels using Indelligent 1.2 (dmitriev.speciesfile.org/indel.asp). If the multiple peaks could be resolved in this way, the majority sequence was associated with that sample. If multiple peaks were not explained by such "indel analysis," chromatograms were characterized by no more than two peaks at each nucleotide location, and multiple peak locations clearly showed a predominant and lesser abundance of called nucleotide, then these predominant and lesser calls were used to identify a primary and secondary sequence, respectively. In this case, the primary sequence was associated with the sample. In cases where multiple-peaked chromatograms could not be explained by indel analysis or by identifying primary and secondary sequences, the sample genotype was not used in further analysis (1 out of 10 samples).

Nine samples that successfully returned *psbA*^{ncr} sequences were aligned manually with additional sequences from the *psbA*^{ncr} alignment created by Hume et al., 2015 (13) that contained sequences from corals collected within the PAG and C3 radiation sequences (17) collected external to the PAG.

Phylogenetic analysis was conducted by Bayesian inference using Mr. Bayes 3.2.2 (mrbayes.sourceforge.net/). Phylogenies were estimated using the Jukes–Cantor (JC) model with a gamma-shaped distribution (+G) with invariable sites (I) (according to Akaike Information Criterion using MEGA6; www.megasoftware.net/). Markov chain Monte Carlo (MCMC) analyses were run for 2.0×10^6 generations (SDs of split frequencies < 0.05), sampling every 1,000 generations. A relative burn-in of 0.25 was used in calculating a 50% majority rule consensus tree.

To compare *psbA*^{ncr} genetic diversity between the *S. thermophilum* group and the two most divergent ITS2 types (C40 and C27) that resolve within the C3-radiation *psbA*^{ncr} phylogeny, as well as between *S. thermophilum* group sequences found within and external to the PAG, pairwise genetic distances and within-group genetic distance were calculated in MEGA6 using the JC model +G (Table S4). Variance was determined to be equal (*F* test) before conducting a two sample Student's *t* test to compare the within-group genetic distances of the samples from sites internal and external to the PAG.

Taxonomic Position of *S. thermophilum* Group Within *Symbiodinium* Clade C. To elucidate the taxonomic position of the *S. thermophilum* group within clade C, a selection of *S. thermophilum* group, ITS2 type C3, and C41 and C39 (two of the top four numerically common subclades) harboring corals (including some corals under culture at the Coral Reef Laboratory Experimental Mesocosm Facility) (34) had their symbiont complement genotyped with six additional genetic markers (35): the nuclear ribosomal large subunit (nr28S), the nuclear elongation factor 2 (*elf2*), the chloroplastic ribosomal large subunit (cp23S) domain V, the coding region of the plastid-encoded photosystem II protein D1 (*psbA*^{cds}), the mitochondrial cytochrome oxidase I (*coi*), and the mitochondrial cytochrome *b* (*cob*). To assess fine-scale taxonomic resolution, the *psbA*^{ncr} was also amplified.

Specifically, the following coral samples underwent this additional genotyping: all samples in the Gulf of Oman and the Red Sea characterized as *S. thermophilum* by *psbA*^{ncr} genotype and containing >99% clade C ITS2 sequences (eight samples); a selection of 23 samples collected in the PAG as part of studies by Hume et al., 2015 (13) and D'Angelo et al., 2015 (15), representing samples collected over >400 km within the PAG and as resolving in different positions within the *psbA*^{ncr} phylogeny of D'Angelo et al., 2015 (15); samples collected in the Red Sea and Gulf of Oman harboring ITS2 type C3 as their numerically dominant ITS2 amplicon and containing no *S. thermo.*-indel amplicons (three samples; OMD001, OMD002, and YBA008; Table S3); three ITS2-type C3-harboring *Euphyllia* spp. corals currently in culture at the Coral Reef Laboratory Experimental Mesocosm Facility (34) but originating from Indo-Pacific waters in proximity to Bali (EU2, EU3, and EU4; Table S3); and finally, four corals containing predominant ITS2 variants for C41 and C39 (representing the first and fourth most common ITS2 variants sampled, respectively) collected in the Red Sea and the Gulf of Oman (Table S3).

All PCR conditions were as for the SYM_VAR_FWD/SYM_VAR_REV primer pair with cycles as detailed in Pochon et al., 2014 (35), except for the *psbA*^{ncr} region that was amplified according to Hume et al., 2015 (13). Sequences were attained through direct PCR sequencing, services provided by Eurofins, using forward (*elf2*, *psbA*^{cds}, *coi*, and *cob*) and reverse (nr28S and cp23S) primers. Sequences from this study were added to a selection of reference sequences (Table S5) representing members from clades A–I, including subcladal C1, C15, C90, and C91, as well as sequence collections from *Gymnodinium simplex* and *Polarella glacialis* as outgroups.

Sequences returned from the six additional genetic markers (i.e., not *psbA*^{ncr}) were aligned in MEGA 6 with the ClustalW algorithm and checked by eye. Hypervariable regions that prevented robust alignment were removed from the cp23S alignment *sensu* Pochon et al., 2006 (16). Phylogenies were estimated both from individual markers and from a concatenated supermatrix of all six markers. Phylogenies were estimated by Bayesian Inference in Mr. Bayes 3.2.2 using the following nucleotide substitution models: nr28S, Kimura 2-Parameter (K2) +G; *Elf2*, K2 +G +I; cp23S, Hasegawa Kishino Yano (HKY) +G; *psbA*^{cds}, Generalized Time Reversible +G; *coi*, HYK +G; *cob*, HKY +G. The supermatrix analysis was partitioned with the separate nucleotide models being used for each marker's region. MCMC analyses were run for 1.0×10^6 generations, sampling every 500 generations. A relative burn-in of 0.25 was used in calculating a 50% majority rule consensus tree. Alignments of the *psbA*^{ncr} sequences returned from the ITS2 type C3 (non-*S. thermo.*-indel–containing), C41, and C39 samples were not possible between ITS2 types from this study and with previous alignments by Hume et al., 2015 (13) (C3/*S. thermophilum* radiation) and Thornhill et al., 2014 (17) (C1 radiation) due to the dissimilarity of the sequences.

ACKNOWLEDGMENTS. We appreciate the help of Cornelia Roder, Sergey Dobretsov, Julia Schnetzer, Todd LaJeunesse, and Drew Wham with sample collection. A. Al-Hemeri (UAE Federal Environment Agency), A. Al-Cibahy (Environment Agency of Abu Dhabi), and the Oman Ministry of Environment & Climate Affairs kindly provided Convention on International Trade in Endangered Species of Wild Fauna and Flora (CITES) export permits (no. 09FEA555) and collection permits. We acknowledge Tropical Marine Centre (London) and Tropic Marin (Wartenberg) for sponsoring the Coral Reef Laboratory at the University of Southampton. We thank the NYU Abu Dhabi Institute for supporting the 2012/2013 field workshops during which samples for this study were collected and the Interuniversity Institute for Marine Sciences in Eilat for field work support. The study was funded by Natural Environment Research Council Grant NE/K00641X/1 (to J.W.), the European Research Council under the European Union's Seventh Framework Programme Grant FP7/2007-2013/ERC Grant Agreement 311179 (to J.W.), the King Abdullah University of Science and Technology (C.R.V.), and Israel Science Foundation Grant 341/12, United States Agency for International Development/Middle East Regional Cooperation (USAID/MERC) No. M32-037 (to Y.L.).

1. Hughes TP, et al. (2003) Climate change, human impacts, and the resilience of coral reefs. *Science* 301(5635):929–933.
2. Palumbi SR, Barshis DJ, Traylor-Knowles N, Bay RA (2014) Mechanisms of reef coral resistance to future climate change. *Science* 344(6186):895–898.
3. Logan CA, Dunne JP, Eakin CM, Donner SD (2014) Incorporating adaptive responses into future projections of coral bleaching. *Glob Change Biol* 20(1):125–139.
4. Jones MJ, Berkelmans R (2011) Tradeoffs to thermal acclimation: Energetics and reproduction of a reef coral with heat tolerant *Symbiodinium* type-D. *J Mar Biol* 2011: 185890.
5. Ortiz JC, González-Rivero M, Mumby PJ (2013) Can a thermally tolerant symbiont improve the future of Caribbean coral reefs? *Glob Change Biol* 19(1):273–281.
6. Pettay DT, Wham DC, Smith RT, Iglesias-Prieto R, LaJeunesse TC (2015) Microbial invasion of the Caribbean by an Indo-Pacific coral zooxanthella. *Proc Natl Acad Sci USA* 112(24):7513–7518.
7. Lambeck K (1996) Shoreline reconstructions for the Persian Gulf since the last glacial maximum. *Earth Planet Sci Lett* 142(1):43–57.
8. Riegl B, Purkis S (2012) Adaptations to climatic extremes in the world's hottest sea. *Coral Reefs of the Gulf*, eds Riegl B, Purkis SJ (Springer, Dordrecht, The Netherlands), pp 1–4.
9. Arz HW, Lamy F, Pätzold J, Muller PJ, Prins M (2003) Mediterranean moisture source for an early-Holocene humid period in the northern Red Sea. *Science* 300(5616): 118–121.
10. Parker AG, et al. (2004) Holocene vegetation dynamics in the northeastern Rub' al-Khali desert, Arabian Peninsula: A phytolith, pollen and carbon isotope study. *J Quat Sci* 19(7):665–676.
11. Coles SL (2003) Coral species diversity and environmental factors in the Arabian Gulf and the Gulf of Oman: A comparison to the Indo-Pacific region. *Atoll Res Bull* 507: 1–19.
12. Intergovernmental Panel on Climate Change (2013) Long-term climate change: Projections, commitments and irreversibility. *Climate Change 2013 the Physical Science Basis Working Group 1 Contribution to the Fifth Assessment Report of the Intergovernmental Panel on Climate Change*, eds Stocker TF, et al. (Cambridge Univ Press, New York), pp 1029–1136.
13. Hume BCC, et al. (2015) *Symbiodinium thermophilum* sp. nov., a thermotolerant symbiotic alga prevalent in corals of the world's hottest sea, the Persian/Arabian Gulf. *Sci Rep* 5:8562.
14. Baird AH, Bhagooli R, Ralph PJ, Takahashi S (2009) Coral bleaching: The role of the host. *Trends Ecol Evol* 24(1):16–20.
15. D'Angelo C, et al. (2015) Local adaptation constrains the distribution potential of heat-tolerant *Symbiodinium* from the Persian/Arabian Gulf. *ISME J* 9(12):2551–2560.
16. Pochon X, Montoya-Burgos JI, Stadelmann B, Pawlowski J (2006) Molecular phylogeny, evolutionary rates, and divergence timing of the symbiotic dinoflagellate genus *Symbiodinium*. *Mol Phylogenet Evol* 38(1):20–30.
17. Thornhill DJ, Lewis AM, Wham DC, LaJeunesse TC (2014) Host-specialist lineages dominate the adaptive radiation of reef coral endosymbionts. *Evolution* 68(2):352–367.
18. Sheppard C, et al. (2010) The Gulf: A young sea in decline. *Mar Pollut Bull* 60(1):13–38.
19. LaJeunesse TC, et al. (2014) Ecologically differentiated stress-tolerant endosymbionts in the dinoflagellate genus Symbiodinium (Dinophyceae) Clade D are different species. *Phycologia* 53(4):305–319.
20. Baird AH, Guest JR, Willis BL (2009) Systematic and biogeographical patterns in the reproductive biology of scleractinian corals. *Annu Rev Ecol Evol Syst* 40:551–571.
21. Riegl B (1999) Corals in a non-reef setting in the southern Arabian Gulf (Dubai, UAE): Fauna and community structure in response to recurring mass mortality. *Coral Reefs* 18(1):63–73.
22. Veron JEN, et al. (2009) Delineating the coral triangle. *Galaxea. J Coral Reef Stud* 11(2):91–100.
23. Loya Y, Sakai K, Nakano Y, Van Woesik R (2001) Coral bleaching: The winners and the losers. *Ecol Lett* 4(2):122–131.
24. Riegl B (2001) Inhibition of reef framework by frequent disturbance examples from the Arabian Gulf, South Africa, and the Cayman Islands. *Palaeogeogr Palaeoclimatol Palaeoecol* 175(1):79–101.

25. Hamylton SM, Leon JX, Saunders MI, Woodroffe CD (2014) Simulating reef response to sea-level rise at Lizard Island: A geospatial approach. *Geomorphology* 222:151–161.
26. Dixon GB, et al. (2015) Genomic determinants of coral heat tolerance across latitudes. *Science* 348(6242):1460–1462.
27. van Oppen MJH, Oliver JK, Putnam HM, Gates RD (2015) Building coral reef resilience through assisted evolution. *Proc Natl Acad Sci USA* 112(8):2307–2313.
28. D'Angelo C, Wiedenmann J (2014) Impacts of nutrient enrichment on coral reefs: New perspectives and implications for coastal management and reef survival. *Curr Opin Environ Sustain* 7:82–93.
29. Edinger EN, Jompa J, Limmon GV, Widjatmoko W, Risk MJ (1998) Reef degradation and coral biodiversity in indonesia: Effects of land-based pollution, destructive fishing practices and changes over time. *Mar Pollut Bull* 36(8):617–630.
30. Vega Thurber RL, et al. (2014) Chronic nutrient enrichment increases prevalence and severity of coral disease and bleaching. *Glob Change Biol* 20(2):544–554.
31. Sale PF (2014) Addressing the decline of coral reefs. *Reef Encounter* 29:15–17.
32. Arif C, et al. (2014) Assessing *Symbiodinium* diversity in scleractinian corals via next-generation sequencing-based genotyping of the ITS2 rDNA region. *Mol Ecol* 23(17):4418–4433.
33. Hume B, et al. (2013) Corals from the Persian/Arabian Gulf as models for thermotolerant reef-builders: Prevalence of clade C3 *Symbiodinium*, host fluorescence and *ex situ* temperature tolerance. *Mar Pollut Bull* 72(2):313–322.
34. D'Angelo C, Wiedenmann J (2012) An experimental mesocosm for long-term studies of reef corals. *J Mar Biol Assoc U K* 92(04):769–775.
35. Pochon X, Putnam HM, Gates RD (2014) Multi-gene analysis of *Symbiodinium* dinoflagellates: A perspective on rarity, symbiosis, and evolution. *PeerJ* 2:e394.

Supporting Information

Hume et al. 10.1073/pnas.1601910113

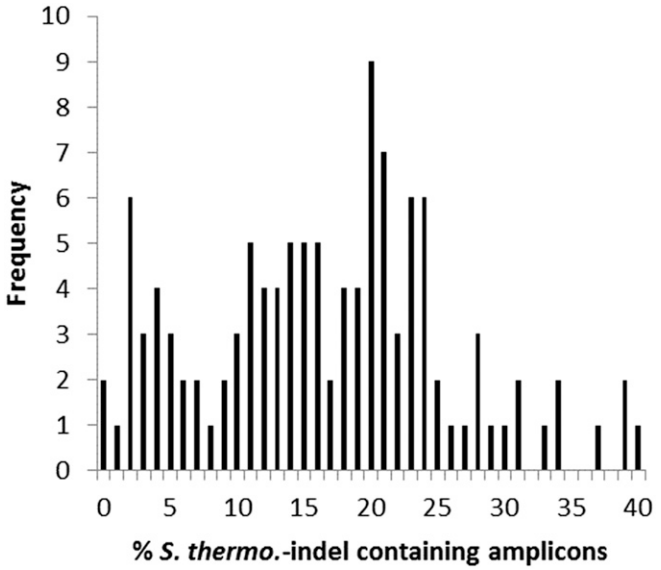

Fig. S1. Proportion of *S. thermo*.-indel–containing variants in total ITS2 sequences from C3 predominated cnidarians (n = 116) from the PAG. Cnidarians included in the analysis contained >50% clade C *Symbiodinium*, of which >95% were C3 or closely related variants. Average % *S. thermo*.-indel–containing amplicons: 16.6%.

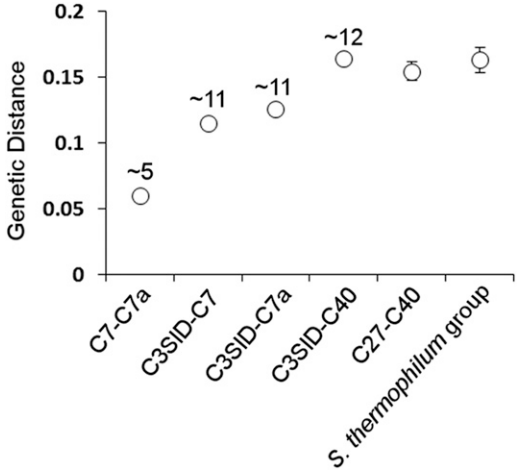

Fig. S2. Estimated age of diversity in the *S. thermophilum* group. C7-C7a, C3SID-C7, C3SID-C7a, and C3SID-C40 represent between-group genetic distance for associated ITS2 groups, with C3SID being defined as the grouping of *Symbiodinium* ITS2 type C3 sequences originating from host *Siderastrea siderea* samples as highlighted in yellow in figure 8A from Thornhill et al., 2014 (17). Numbers above genetic distances represent corresponding lineage diversification ages (Mya) extracted from figure 8A of Thornhill et al., 2014 (17). C27–C40 and *S. thermophilum* group represent average pairwise genetic distances between the five most divergent pairs between ITS2 groups C27 and C40 and within the *S. thermophilum* group. Error bars represent 1 SD above and below the average (comparisons of five most divergent pairs only). Values for all genetic distances as well as details of the five most divergent pairs are given in Table S4.

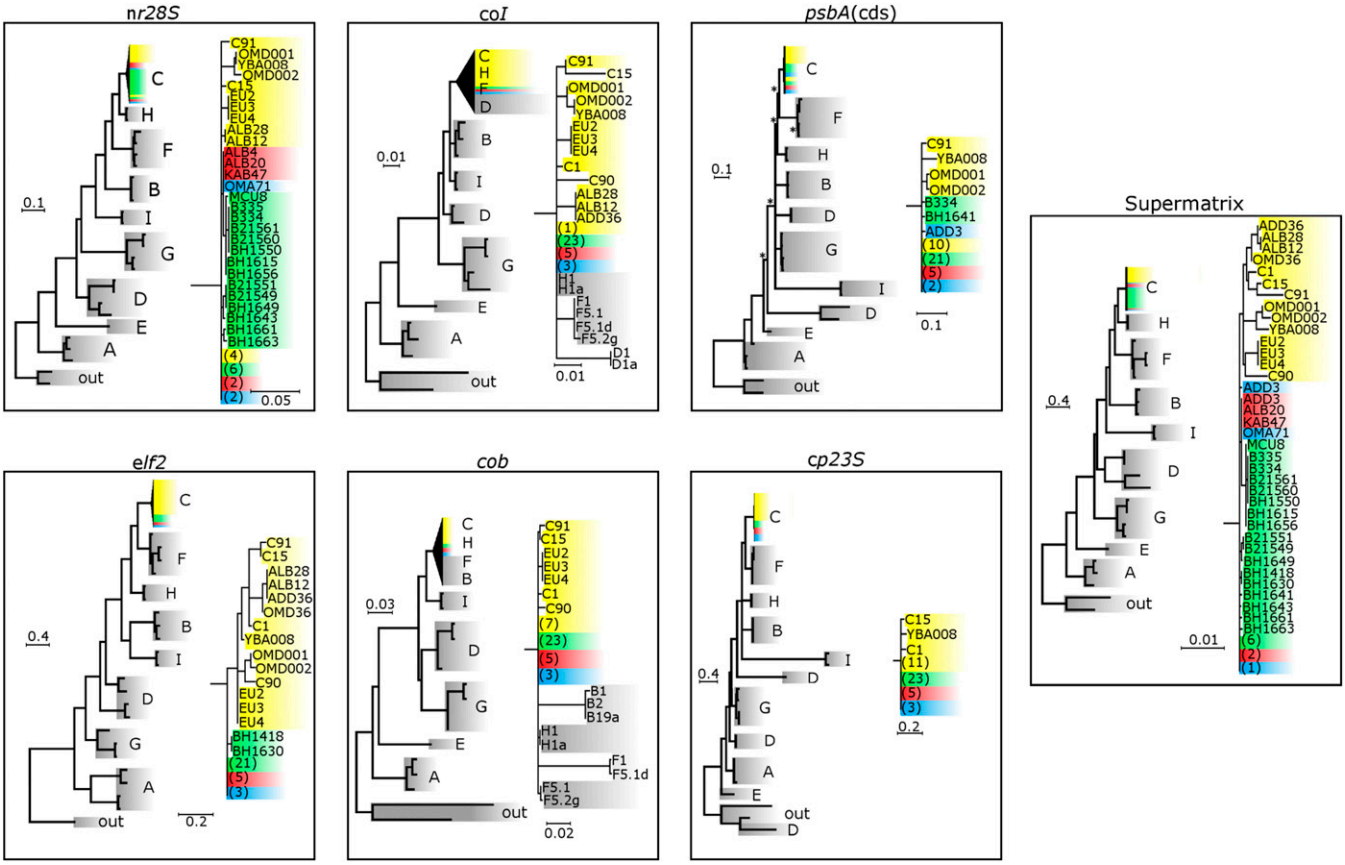

Fig. S3. Rooted single-gene and supermatrix estimated phylogenies for *Symbiodinium* spp. Shown are single-gene and supermatrix estimated phylogenies (Bayesian analysis with nodes support assessed through posterior probabilities) for a suite of A–I clade sequences (gray), including subcladal C sequences (C3, C1, C41, and C39; yellow) and *S. thermophilum* sequences from the PAG (green), Gulf of Oman (blue), and Red Sea (red). For each phylogeny, a full tree is illustrated on the left, in which the clade C subtree is collapsed. The resolution of this collapsed subtree is shown in detail to the right. Numbers in parentheses represent multiple sequences resolving at the same position and are color coded according to collection site and sequence type (Gulf of Oman, blue; PAG, green; Red Sea, red; reference sequence, yellow). Nodes supported with PPs above 0.8 are not displayed. Nodes with supports below 0.8 are marked with an asterisk.

Table S1. Detection of *S. thermophilum* symbionts in the PAG, the Gulf of Oman, and the Red Sea through screening for the rDNA ITS2 *S. thermo.*-indel

Water body	Region (abbreviation)	Reef	Number of samples	% hosts with *S. thermo.*-indel	Hosts >1%* *S. thermo.*-indel	Hosts <1%* *S. thermo.*-indel	Genera with *S. thermo.*-indel
PAG	Jana (JAN)	Subri	31	29	6	3	5 of 13
		Subri (Jana)	41	27	8	3	10 of 18
		Chandelier	23	74	13	4	7 of 9
	Yassat (YAS)	Al Yassat	33	100	33	0	7 of 7
	Saadiyat (SAD)	Saadiyat	42	98	40	1	11 of 12
		Ras Ghanada	26	96	22	3	7 of 7
Gulf of Oman	Fujairah (FUJ)	Al Aqah	34	15	1	4	4 of 14
		Dibba Rock	37	0	0	0	0 of 14
	Muscat (MUS)	Bandar Khayran Islet	90	0	0	0	0 of 21
		Damanyat 3 sisters	35	0	0	0	0 of 17
		Damanyat legends	36	0	0	0	0 of 16
		Damanyat Noodle	58	0	0	0	0 of 15
		Fahal Island Site I	34	6	1	1	2 of 14
		Fahal Island Site II	28	7	1	1	2 of 12
		Saifat Ash Shiekh	87	1	1	0	1 of 23
Red Sea	Eilat (EIL)	Eilat	27	0	0	0	0 of 1
	Yanbu (YAN)	Yanbu 23	31	3	1	0	3 of 13
		Yanbu Ayona	36	0	0	0	0 of 17
	KAUST (KAU)	KAUST Al Fahal	42	0	0	0	0 of 16
		KAUST Inner Fsar	31	3	1	0	2 of 13
		KAUST Shib Nazaar	43	0	0	0	0 of 16
	Al Lith (LIT)	Al Lith Abu Lath	40	15	3	3	7 of 17
		Al Lith South Reef	33	0	0	0	0 of 18

*This is representative of total ITS2 amplicons detected (all clades).

Table S2. Proportion of taxa in which *S. thermophilum* symbionts were detected through screening for the ribosomal DNA ITS2 *S. thermo*.-indel

	Detected		Undetected	
Taxa	Subtaxa	Proportion	Subtaxa	Proportion
Actiniaria	Unidentified	1/3		
	Entacmea	1/1		
Alcyonacea			Unidentified	0/4
Alcyoniidae	*Sarcophyton*	1/11	*Lobophytum*	0/3
	Sinularia	1/4		
Nephtheidae			*Nephthea*	0/1
Xeniidae			*Xenia*	0/23
Scleractinia				
Acroporidae	*Acropora*	12/107	*Astreopora*	0/14
	Montipora	10/56		
Agariciidae	*Pavona*	3/48	*Gardineroseris*	0/5
Astrocoeniidae	*Madracis*	1/2	*Stephanocoenia*	0/0
			Stylocoeniella	0/1
Dendriphyllidae	*Turbinaria*	7/14		
Diploastreidae			*Diploastrea*	0/5
Caryophylliidae			*Cladocora*	0/1
Coscinaraeidae	*Coscinaraea*	1/4		
Fungiidae			*Fungia*	0/7
Lobophyllidae	*Acantastrea*	2/9	*Echinophyllia*	0/12
Merulinidae	*Cyphastrea*	26/42	*Echinopora*	0/20
	Favites	9/40	*Hydnophora*	0/6
	Goniastrea	1/15	*Oulophyllia*	0/1
	Leptoria	2/4		
	Platygyra	16/53		
Montastraeidae			*Montastraea*	0/1
Mussidae	*Favia*	20/60	*Symphyllia*	0/9
	Leptastrea	2/26		
	Unidentified	1/1		
Oculinidae	*Galaxea*	1/8		
Pectiniidae			*Mycedium*	0/1
Pocilloporidae	*Pocillopora*	3/75		
	Seriatopora	1/6		
	Stylophora	3/43		
Poritidae	*Goniopora*	1/18		
	Porites	27/98		
Siderastreidae	*Psammocora*	9/26		
Zoantharia				
Sphenopidae	*Palythoa*	1/1		

Table S3. Accession numbers for the seven genetic markers (amplicons) used in this study

Sample	Location	Region	Type	nr28S	cp23S	*elf2*	*psbA*^{cds}	*coi*	*cob*	*psbA*^{ncr}
ADD036*	Al Aqah	FUJ	C39	KR996268	KR996350	KR996309	KR996391	KR996432	KR996473	KT156647
OMD036*	SAS[†]	MUS	C39	KR996269	KR996351	KR996310	KR996392	KR996433	KR996474	KT156648
ALB028*	Al Lith	LIT	C41	KR996270	KR996352	KR996311	KR996393	KR996434	KR996475	KT156649
ALB012*	Al Lith	LIT	C41	KR996271	KR996353	KR996312	KR996394	KR996435	KR996476	KT156650
OMD001*	SAS	MUS	C3	KR996272	KR996354	KR996313	KR996395	KR996436	KR996477	KT156651
OMD002*	SAS	MUS	C3	KR996273	KR996355	KR996314	KR996396	KR996437	KR996478	KT156652
YBA008*	Yanbu	YAN	C3	KR996274	KR996356	KR996315	KR996397	KR996438	KR996479	KT156653
ADD3*	Al Aqah	FUJ	Group[‡]	KR996275	KR996357	KR996316	KR996398	KR996439	KR996480	KT156654
ALB4*	Al Lith	LIT	Group	KR996276	KR996358	KR996317	KR996399	KR996440	KR996481	KT156655
ALB20*	Al Lith	LIT	Group	KR996277	KR996359	KR996318	KR996400	KR996441	KR996482	KT156656
KAB47*	KAUST	KAU	Group	KR996278	KR996360	KR996319	KR996401	KR996442	KR996483	KT156657
OMD54*	SAS	MUS	Group	KR996279	KR996361	KR996320	KR996402	KR996443	KR996484	KT156658
YBA16*	Yanbu	YAN	Group	KR996280	KR996362	KR996321	KR996403	KR996444	KR996485	KT156659
ALB30*	Al Lith	LIT	Group	KR996281	KR996363	KR996322	KR996404	KR996445	KR996486	KT156660
OMA71*	Fahal Isl.	MUS	Group	KR996282	KR996364	KR996323	KR996405	KR996446	KR996487	KT156661
ADD014*	Al Aqah	FUJ	Group	N/A	N/A	N/A	N/A	N/A	N/A	KT156662
EU2*	Bali	N/A	C3	KR996283	KR996365	KR996324	KR996406	KR996447	KR996488	KT156663
EU3*	Bali	N/A	C3	KR996284	KR996366	KR996325	KR996407	KR996448	KR996489	KT156664
EU4*	Bali	N/A	C3	KR996285	KR996367	KR996326	KR996408	KR996449	KR996490	KT156665
BH21551	MP	N/A	Group	KR996286	KR996368	KR996327	KR996409	KR996450	KR996491	KP280292
BH1660[§]	UAQ	N/A	Group	KR996287	KR996369	KR996328	KR996410	KR996451	KR996492	KP280262
BH1665[§]	UAQ	N/A	Group	KR996288	KR996370	KR996329	KR996411	KR996452	KR996493	KP280251
BH1643[§]	Dalma	N/A	Group	KR996289	KR996371	KR996330	KR996412	KR996453	KR996494	KP280213
BH1661[§]	UAQ	N/A	Group	KR996290	KR996372	KR996331	KR996413	KR996454	KR996495	KP280263
B21549[§]	MP	N/A	Group	KR996291	KR996373	KR996332	KR996414	KR996455	KR996496	KP280287
BH1659[§]	MP	N/A	Group	KR996292	KR996374	KR996333	KR996415	KR996456	KR996497	KP280300
BH1699[§]	Saadiyat	N/A	Group	KR996293	KR996375	KR996334	KR996416	KR996457	KR996498	KP280227
BH1663[§]	UAQ	N/A	Group	KR996294	KR996376	KR996335	KR996417	KR996458	KR996499	KP280264
B335[§]	Muscat	N/A	Group	KR996295	KR996377	KR996336	KR996418	KR996459	KR996500	KP280311
B334[§]	Al Aqah	N/A	Group	KR996296	KR996378	KR996337	KR996419	KR996460	KR996501	KP280310
BH1615[§]	MP	N/A	Group	KR996297	KR996379	KR996338	KR996420	KR996461	KR996502	KP280306
BH1693[§]	Dalma	N/A	Group	KR996298	KR996380	KR996339	KR996421	KR996462	KR996503	KP280218
B21561[§]	Al Aqah	N/A	Group	KR996299	KR996381	KR996340	KR996422	KR996463	KR996504	KP280307
BH1694[§]	Saadiyat	N/A	Group	KR996300	KR996382	KR996341	KR996423	KR996464	KR996505	KP280224
BH1656[§]	MP	N/A	Group	KR996301	KR996383	KR996342	KR996424	KR996465	KR996506	KP280304
B21560[§]	Al Aqah	N/A	Group	KR996302	KR996384	KR996343	KR996425	KR996466	KR996507	KP280309
BH1550[§]	Al Aqah	N/A	Group	KR996303	KR996385	KR996344	KR996426	KR996467	KR996508	KP280308
BH1418[§]	Saadiyat	N/A	Group	KR996304	KR996386	KR996345	KR996427	KR996468	KR996509	KP280238
BH1630[§]	UAQ	N/A	Group	KR996305	KR996387	KR996346	KR996428	KR996469	KR996510	KP280257
BH1649[§]	MP	N/A	Group	KR996306	KR996388	KR996347	KR996429	KR996470	KR996511	KP280296
BH1641[§]	Saadiyat	N/A	Group	KR996307	KR996389	KR996348	KR996430	KR996471	KR996512	KP280233
B359[§]	Saadiyat	N/A	Group	KR996308	KR996390	KR996349	KR996431	KR996472	KR996513	KP280223

*Samples were collected as part of this study.
[†]Locations were as follows: MP, Musandam Peninsular; UAQ, Umm Al Quwain; SAS, Saifat Ash Shiekh.
[‡]The group is *S. thermophilum*.
[§]Samples were collected and *psbA*^{ncr} sequences were amplified as part of D'Angelo et al., 2015 (15).

Table S4. Pairwise and average between- and within-group genetic distances based on the *psbA*^{ncr} alignment from this study*

Sequence/group 1	Sequence/group 2	Genetic distance
S. thermophilum		Average, 0.163
ALB30[†] (Al Lith)	BH1428 (Umm Al Quwain)	0.155
BH1660 (Umm Al Quwain)	BH1693 (Dalma)	0.156
B335 (Muscat)	BH1633 (Ras Ghanada)	0.160
B21557 (Musandam)	B315 (Saadiyat)	0.167
B21561 (Fujairah)	BH1642 (Saadiyat)	0.178
C40 and C27		Average, 0.154
C27J043670	C40K572369	0.147
C27J043674	C40K572361	0.147
C27J043669	C40K572360	0.157
C27J043671	C40K572365	0.158
C27J043668	C40K572367	0.163
Between group		
C3SID	C40	0.164
C3SID	C7a	0.126
C3SID	C7	0.115
C7	C7a	0.060
S. thermophilum (PAG)		0.039
S. thermophilum (external)		0.065

*Pairwise genetic distances of the five most disparate pairs within the *S. thermophilum* group and between the ITS2 type C40 and C27 groups are shown under the first two corresponding subheadings. Between-group genetic distance of three ITS2 groups (C40, C7, and C7a) and a monophyletic group of *Symbiodinium* ITS2 type C3 sequences originating from host *S. siderea* samples (C3SID) as highlighted in yellow in figure 8A from Thornhill et al., 2014 (17) are shown under the subheading "Between group." Finally, average within-group genetic distances of *S. thermophilum* group samples from the PAG and external to the PAG are shown. A partial graphical representation of the data is shown in Fig. S2. Sampling locations are detailed in parentheses.

[†]Sequences were obtained in this study. All other *S. thermophilum* group sequences were acquired as part of D'Angelo et al., 2015 (15) or Hume et al., 2015 (13).

Table S5. Reference sequences used in the single-gene and supermatrix estimations of phylogeny

ITS2	nr28S	cp23S	*elf2*	*psbA*^{cds}	*coi*	*cob*
C1	JN558040	JN557969	JN557869	JN557844	JN557891	JN557943
C15	JN558042	JN557972	JN557870	JN557845	JN557892	JN557944
C90	JN558045	JN557975	JN557871	JN557846	JN557893	JN557945
C91	JN558048	JN557978	JN557872	JN557847	JN557894	JN557944
H1	JN558051	JN557981	JN557873	JN557848	JN557895	JN557947
H1a	JN558053	JN557984	JN557874	JN557849	JN557896	JN557948
F1	JN558066	JN557996	JN557875	JN557850	JN557897	JN557949
F5.1	JN558063	JN557996	JN557876	JN557851	JN557898	JN557950
F5.1d	JN558066	JN558000	JN557877	JN557852	JN557899	JN557951
F5.2g	JN558072	JN558004	JN557878	JN557853	JN557900	JN557952
B1	JN558057	JN557991	JN557879	JN557854	JN557901	JN557953
B2	JN558060	JN557993	JN557880	JN557855	JN557902	JN557954
B19a	JN558055	JN557987	JN557880	JN557856	JN557903	JN557955
I1	FN561559	FN561563	JQ277955	JQ277944	JQ277966	JQ277988
I2	FN561560	FN561564	JQ277956	JQ277945	JQ277967	JQ277989
D1	JN558075	JN558007	JN557882	JN557857	JN557904	JN557956
D1a	JN558078	JN558010	JN557883	JN557858	JN557905	JN557957
D1.1	JQ247049	JQ247058	JQ277952	JQ277941	JQ277963	JQ277985
D1.2	JN558078	JN558013	JN557884	JN557859	JN557906	JN557958
G2	JN558081	JN558019	JQ277953	JN557860	JN557907	JN557959
G2b	JN558089	JN558017	N/A	JN557861	JN557908	JN557960
G2.1	JQ247050	JQ247059	JQ277953	JQ277942	JQ277964	JQ277986
G2.2	JQ247051	JQ247060	JQ277954	JQ277943	JQ277965	JQ277987
E1	JN558084	JN558015	N/A	JN557862	JN557909	JN557961
A2	JN558097	JN558029	JN557887	JN557864	JN557911	JN557963
A3	JN558094	JN558021	JN557889	JN557866	JN557913	JN557965
A13	JN558094	JN558027	JN557886	JN557863	JN557910	JN557962
G. simplex	JN558103	JN558033	JN557890	JN557867	JN557914	JN557966
P. glacialis	JN558108	JN558036	N/A	JN557868	JN557916	JN557968

Table S6. Phylogenetic differentiation of taxa from the clade C ancestral nodes in single-gene phylogenies

Sample	ITS2 type	nr28S	*elf2*	*coi*	*psbA*^{cds}	*cob*	cp23S	Supermatrix	Total
C91	C91	1*	1	1	1	1	0†	1	5
OMD001	C3	1	1	1	1	0	0	1	4
OMD002	C3	1	1	1	1	0	0	1	4
C15	C15	1	1	1	0	1	0	1	4
YBA008	C3	1	1	1	1	0	0	1	4
EU2	C3	1	1	1	0	0	0	1	4
EU3	C3	1	1	1	0	0	0	1	4
EU4	C3	1	1	1	0	0	0	1	4
C1	C1	0	1	1	0	1	0	1	3
C90	C90	0	1	1	0	1	0	1	3
ALB028	C41	1	1	1	0	0	0	1	3
ALB012	C41	1	1	1	0	0	0	1	3
ADD036	C39	0	1	1	0	0	0	1	2
B334	*S. thermophilum*	1	0	0	1	0	0	1	2
OMD036	C39	0	1	0	0	0	0	1	1
BH1418	*S. thermophilum*	0	1	0	0	0	0	1	1
BH1630	*S. thermophilum*	0	1	0	0	0	0	1	1
BH1641	*S. thermophilum*	0	0	0	1	0	0	1	1
ADD003	*S. thermophilum*	0	0	0	1	0	0	1	1
ALB004	*S. thermophilum*	1	0	0	0	0	0	1	1
ALB020	*S. thermophilum*	1	0	0	0	0	0	1	1
KAB047	*S. thermophilum*	1	0	0	0	0	0	1	1
OMA071	*S. thermophilum*	1	0	0	0	0	0	1	1
BH1659	*S. thermophilum*	1	0	0	0	0	0	1	1
B335	*S. thermophilum*	1	0	0	0	0	0	1	1
B21561	*S. thermophilum*	1	0	0	0	0	0	1	1
B21560	*S. thermophilum*	1	0	0	0	0	0	1	1
BH1550	*S. thermophilum*	1	0	0	0	0	0	1	1
BH1615	*S. thermophilum*	1	0	0	0	0	0	1	1
BH1656	*S. thermophilum*	1	0	0	0	0	0	1	1
B21551	*S. thermophilum*	1	0	0	0	0	0	1	1
BH21549	*S. thermophilum*	1	0	0	0	0	0	1	1
BH1649	*S. thermophilum*	1	0	0	0	0	0	1	1
BH1643	*S. thermophilum*	1	0	0	0	0	0	1	1
BH1661	*S. thermophilum*	1	0	0	0	0	0	1	1
BH1663	*S. thermophilum*	1	0	0	0	0	0	1	1
OMD054	*S. thermophilum*	0	0	0	0	0	0	0	0
YBA016	*S. thermophilum*	0	0	0	0	0	0	0	0
ALB030	*S. thermophilum*	0	0	0	0	0	0	0	0
BH1660	*S. thermophilum*	0	0	0	0	0	0	0	0
BH1660	*S. thermophilum*	0	0	0	0	0	0	0	0
BH1699	*S. thermophilum*	0	0	0	0	0	0	0	0
BH1693	*S. thermophilum*	0	0	0	0	0	0	0	0
BH1694	*S. thermophilum*	0	0	0	0	0	0	0	0
B359	*S. thermophilum*	0	0	0	0	0	0	0	0

*For each sample, a "1" in a single-gene column denotes the sample was not resolved on the clade C ancestral node of that phylogeny.

†"0" denotes resolution on the ancestral node.

Table S7. Sequences included in the calculation of within-group (PAG vs. Gulf of Oman/Red Sea) genetic distance

ID	Collection site	Accession number	Host taxon	ID	Collection site*	Accession number	Host taxon
Persian/Arabian Gulf sequences				Persian/Arabian Gulf sequences			
BH1415	Dalma	KM458276[†]	*Porites harrisoni*	BH1630	Umm Al Quwain	KP280257	*P. lutea*
BH1686	Dalma	KP280207	*P. harrisoni*	BH1668	Umm Al Quwain	KP280258	*P. lutea*
BH1448	Dalma	KM458286	*P. harrisoni*	BH1456	Umm Al Quwain	KM458291	*P. lutea*
BH1413	Dalma	KM458274	*P. harrisoni*	BH1626	Umm Al Quwain	KP280259	*P. lutea*
BH1684	Dalma	KP280208	*P. harrisoni*	BH1669	Umm Al Quwain	KP280260	*P. lutea*
BH1414	Dalma	KM458275	*P. harrisoni*	BH1457	Umm Al Quwain	KP280261	*P. lutea*
BH1685	Dalma	KP280209	*P. harrisoni*	BH1660	Umm Al Quwain	KP280262	*P. lutea*
BH1450	Dalma	KM458288	*Porites lutea*	BH1392	Umm Al Quwain	KM458294	*P. lutea*
BH1449	Dalma	KM458287	*P. lutea*	BH1661	Umm Al Quwain	KP280263	*P. lutea*
BH1689	Dalma	KP280210	*P. lutea*	BH1458	Umm Al Quwain	KM458292	*P. lutea*
BH1692	Dalma	KP280211	*P. lutea*	BH1427	Umm Al Quwain	KM458284	*P. lutea*
BH1690	Dalma	KP280212	*P. harrisoni*	BH1663	Umm Al Quwain	KP280264	*P. lutea*
BH1643	Dalma	KP280213	*P. harrisoni*	BH1679	Umm Al Quwain	KP280265	*P. lutea*
BH1411	Dalma	KM458273	*P. harrisoni*	BH1688	Umm Al Quwain	KP280266	*P. lutea*
BH1647	Dalma	KP280215	*P. harrisoni*	BH1675	Ras Al Kaimah	KP280267	*Porites sp.*
BH1691	Dalma	KP280216	*P. harrisoni*	BH1621	Ras Al Kaimah	KP280268	*Porites sp.*
BH1447	Dalma	KP280217	*P. harrisoni*	BH1671	Ras Al Kaimah	KP280269	*Porites sp.*
BH1693	Dalma	KP280218	*P. lutea*	BH1672	Ras Al Kaimah	KP280270	*Porites sp.*
BH1416	Dalma	KP280219	*P. harrisoni*	BH1676	Ras Al Kaimah	KP280271	*Porites sp.*
BH1702	Saadiyat	KP280220	*Porites lobata*	BH1623	Ras Al Kaimah	KP280272	*Porites sp.*
BH1704	Saadiyat	KP280221	*P. lobata*	BH1620	Ras Al Kaimah	KP280273	*Porites sp.*
BH1708	Saadiyat	KP280222	*P. lobata*	BH1624	Ras Al Kaimah	KP280275	*Porites sp.*
BH1356	Saadiyat	KM458293	*P. lutea*	BH1670	Ras Al Kaimah	KP280276	*Porites sp.*
B359	Saadiyat	KP280223	*P. lutea*	BH1673	Ras Al Kaimah	KP280277	*Porites sp.*
BH1422	Saadiyat	KM458279	*P. lutea*	BH1678	Ras Al Kaimah	KP280278	*Porites sp.*
BH1694	Saadiyat	KP280224	*P. lutea*	BH1680	Ras Al Kaimah	KP280279	*Porites sp.*
BH1451	Saadiyat	KM458289	*P. lobata*	BH1677	Ras Al Kaimah	KP280280	*Porites sp.*
BH1695	Saadiyat	KP280225	*P. lobata*	BH1683	Ras Al Kaimah	KP280281	*Porites sp.*
BH1417	Saadiyat	KM458277	*P. lutea*	BH1497	Ras Al Kaimah	KP280282	*Porites sp.*
BH1419	Saadiyat	KM458278	*P. lutea*	BH1625	Ras Al Kaimah	KP280283	*Porites sp.*
BH1640	Saadiyat	KP280226	*P. lobata*	BH1682	Ras Al Kaimah	KP280284	*Porites sp.*
BH1699	Saadiyat	KP280227	*P. lutea*	BH1681	Ras Al Kaimah	KP280285	*Porites sp.*
BH1701	Saadiyat	KP280228	*P. lutea*	BH1674	Ras Al Kaimah	KP280286	*Porites sp.*
BH1705	Saadiyat	KP280229	*P. lutea*	B21549	Musandam[‡]	KP280287	*P. lobata*
BH1706	Saadiyat	KP280230	*P. lutea*	B21550	Musandam[‡]	KP280288	*P. lobata*
B315	Saadiyat	KP280231	*P. harrisoni*	BH1652	Musandam[‡]	KP280289	*P. lobata*
BH1696	Saadiyat	KP280232	*P. harrisoni*	BH1616	Musandam[‡]	KP280290	*P. lutea*
BH1641	Saadiyat	KP280233	*P. lobata*	BH1617	Musandam[‡]	KP280291	*P. lobata*
BH1703	Saadiyat	KP280234	*P. harrisoni*	B21551	Musandam[‡]	KP280292	*P. lutea*
BH1642	Saadiyat	KP280235	*P. harrisoni*	B21552	Musandam[‡]	KP280293	*P. lutea*
BH1698	Saadiyat	KP280236	*P. lutea*	B21553	Musandam[‡]	KP280294	*P. lutea*
BH1487	Saadiyat	KP280237	*P. lobata*	B21554	Musandam[‡]	KP280295	*P. lutea*
BH1418	Saadiyat	KP280238	*P. lutea*	BH1649	Musandam[‡]	KP280296	*P. lobata*
BH1639	Saadiyat	KP280239	*P. lutea*	BH1653	Musandam[‡]	KP280297	*P. lutea*
BH1700	Saadiyat	KP280240	*P. harrisoni*	BH1655	Musandam[‡]	KP280298	*P. lutea*
BH1453	Saadiyat	KM458290	*P. lobata*				
BH1697	Saadiyat	KP280241	*P. lobata*	Gulf of Oman and Red Sea sequences			
BH1636	Ras Ghanada	KP280242	*P. lutea*	B341	Musandam[§]	KP280299	*P. lutea*
BH1547	Ras Ghanada	KP280243	*P. lobata*	BH1659	Musandam[§]	KP280300	*P. lutea*
BH1632	Ras Ghanada	KP280244	*P. lobata*	B21556	Musandam[§]	KP280301	*P. lobata*
BH1634	Ras Ghanada	KP280245	*P. harrisoni*	BH1658	Musandam[§]	KP280302	*P. lobata*
BH1635	Ras Ghanada	KP280246	*P. harrisoni*	B21557	Musandam[§]	KP280303	*P. lobata*
BH1548	Ras Ghanada	KP280247	*P. lutea*	BH1656	Musandam[§]	KP280304	*P. lobata*
BH1631	Ras Ghanada	KP280248	*P. harrisoni*	BH1614	Musandam[§]	KP280305	*P. lobata*
BH1633	Ras Ghanada	KP280249	*P. harrisoni*	BH1615	Musandam[§]	KP280306	*P. lobata*
BH1664	Umm Al Quwain	KP280250	*P. lutea*	B21561	Fujairah	KP280307	*P. lobata*
BH1425	Umm Al Quwain	KM458282	*P. lutea*	BH1550	Fujairah	KP280308	*P. lobata*
BH1665	Umm Al Quwain	KP280251	*P. lutea*	B21560	Fujairah	KP280309	*P. lobata*
BH1662	Umm Al Quwain	KP280252	*P. lutea*	B334	Fujairah	KP280310	*P. lobata*
BH1428	Umm Al Quwain	KM458285	*P. lutea*	B335	Muscat	KP280311	*Porites sp.*
BH1627	Umm Al Quwain	KP280253	*P. lutea*	ADd014	Fujairah AA	KT156662	*Galxea*
BH1424	Umm Al Quwain	KM458281	*P. lutea*	ADd003	Fujairah AA	KT156654	*Leptastrea*

Table S7. Cont.

ID	Collection site	Accession number	Host taxon	ID	Collection site*	Accession number	Host taxon
BH1666	Umm Al Quwain	KP280254	*P. lutea*	ALb020	Al Lith ALS	KT156656	*Montipora.*
BH1628	Umm Al Quwain	KP280255	*P. lutea*	ALb030	Al Lith ALS	KT156660	*Montipora*
BH1426	Umm Al Quwain	KM458283	*P. lutea*	ALb004	Al Lith ALS	KT156655	*Montipora*
BH1629	Umm Al Quwain	KP280256	*P. lutea*	KAb047	KAUST KIF	KT156657	*Montipora*
BH142	Umm Al Quwain	KM458280	*P. lutea*	OMa071	Muscat FIS2	KT156661	*Palythoa*
				OMd054	Muscat SAS	KT156658	*Goniastrea*
				YBa016	Yanbu Y23	KT156659	*Montipora*

*Collection site abbreviations are as follows: AA, Al Aqah; ALS, Abu lath Shallow Reef; FIS2, Fahal Island Site 2; KIF, KAUST Inner Fasr; SAS, Saifat Ash Shiekh; Y23, Yanbu 23.

†Sequence accessions beginning with KM are from Hume et al., 2015 (13), beginning with KP are from D'Angelo et al., 2015 (15), and beginning with KT are from this study.

‡From samples collected on the PAG side of the Musandam peninsula.

§From samples collected on the Gulf of Oman side of the Musandam peninsula.